RNA Molecules That Specifically and Stoichiometrically Bind Aminoglycoside Antibiotics with High Affinities[†]

Yong Wang, Jennifer Killian, Keita Hamasaki, and Robert R. Rando*

Department of Biological Chemistry and Molecular Pharmacology, Harvard Medical School, 250 Longwood Avenue, Boston, Massachusetts 02115

Received April 11, 1996; Revised Manuscript Received July 2, 1996[⊗]

ABSTRACT: RNA aptamers had previously been selected which were able to bind to the aminoglycoside antibiotic tobramycin with high affinity (Wang & Rando, 1995). Consensus sequences are found in a variety of constructs, and these sequences were mapped to stem-loop regions by Mfold secondary structure prediction. A tobramycin-based affinity cleavage reagent specifically cleaves the aptamers in their consensus regions. A fluorescence depolarization method is developed to accurately measure the affinity and stoichiometry of aminoglycoside binding to RNA constructs. An RNA aptamer (J6RNA) selected to bind to the aminoglycoside antibiotic tobramycin is shown to do so with an affinity of 0.77 nM and a stoichiometry of 1:1. (Fluorescently labeled) 5-carboxytetramethylrhodamine tobramycin (CRT) is used as a ligand in the fluorescence depolarization studies. J6RNA binding is quite specific for tobramycin, and weakly binds structurally related aminoglycosides with affinities 10^3-10^4-fold lower than that for tobramycin. Specific aminoglycoside binding aptamers of this type should be useful for revealing the rules of RNA−aminoglycoside recognition.

RNA is able to achieve intricate three-dimensional structures which can have dynamic biological functions. An extraordinary example of this appears in the case of ribozymes (Cech, 1990; Altman, 1989). Furthermore, studies on the selection of random pools of RNA with relatively specific small-molecule binding capacities (aptamers) support the idea that RNA is capable of forming active-site structures reminiscent of proteins (Ellington et al., 1990; Tuerk & Gold, 1990; Beaudry & Joyce, 1992). If this hypothesis is generally true, then it ought to be possible to design specific antagonists of functional RNA molecules, just as one can for protein enzymes and receptors. In fact, nature has already provided antibiotic molecules which can interact specifically with particular RNA molecules. A straightforward example of this is the case of aminoglycoside antibiotics, which preferentially interfere with procaryotic rRNA function during protein biosynthesis (Woodcock et al., 1991). It would be of some interest to determine what the rules are for specific RNA−aminoglycoside interactions, so that one could begin to design aminoglycoside analogs specific for a particular RNA structure. Toward this end, we have begun to apply selection techniques (Ellington & Szostak, 1990; Tuerk & Gold, 1990; Beaudry & Joyce, 1992) to generate RNA molecules which specifically recognize particular aminoglycosides with high affinity (Wang & Rando, 1995). It is of substantial interest to generate RNA molecules specific for a particular aminoglycoside, and then to determine which structural features of the RNA molecule are important for binding. In previous studies, consensus sequences were uncovered for high affinity tobramycin binding aptamers (Wang & Rando, 1995). Secondary structural predictions suggested that the consensus regions were confined to stem-loop structures (Wang & Rando, 1995). It is shown here that these stem-loop structures comprise an important part of the aminoglycoside binding site. This is demonstrated by affinity cleavage techniques. A further important aim of this work is to produce new quantitative tools which can be used to analyze the affinity and stoichiometry of binding of aminoglycosides to the cognate RNA molecules. We also show that an RNA construct, referred to as J6RNA (Wang & Rando, 1995), can stoichiometrically bind the aminoglycoside tobramycin with a subnanomolar K_D, and discriminate between related aminoglycosides by factors of 10^3-10^4. These determinations are made possible by the methodology of fluorescence depolarization, using fluorescein- or rhodamine-labeled tobramycin analogs. The nature of the assay is such that it appears to be 150-fold more sensitive than immunofluorescence assays developed to measure tobramycin levels, which typically operate in the micromolar concentration range (Chan, 1987).

MATERIALS AND METHODS

Materials

Tobramycin, neomycin B, gentamycin C, and erythromycin were from Fluka. 5-Carboxyfluorescein succinimidyl ester and 5-carboxytetramethylrhodamine succinimidyl ester were purchased from Molecular Probes. All other chemicals were purchased from Aldrich or Sigma and were of the highest purity available. The T7-MEGAshortscript kit was from Ambion. T4 RNA ligase, RNase U2, and RNase T1 were purchased from Boehringer Mannheim. [5′-^{32}P]Cytidine 3′,5′-bisphosphate was a product of NEN. Sephadex

[†] These studies were partially funded by U.S. Public Health Service National Institutes of Health Grants EY-03624 and EY-04096. J.K was funded by postdoctoral fellowship EY-06634 and K.H. by a research fellowship from the Japan Society for the Promotion of Science.

* To whom correspondence should be addressed.

[⊗] Abstract published in *Advance ACS Abstracts,* August 15, 1996.

S0006-2960(96)00878-1 CCC: $12.00

G-50 gel in NICK columns was a product of Pharmacia.

Methods

Synthesis of 5-Carboxyfluorescein-Labeled Tobramycin (CFT). Tobramycin (100 mg, ca. 214 μmol) was dissolved in water (500 μL), and an equivalent amount of DMF was added to the solution. After cooling to 5 °C, 500 μL of 5-carboxyfluorescein succinimidyl ester DMF solution (10 mg, ca. 21 μmol) was added. The solution was stirred at 5 °C for 1 h. Then 10 mL of water was added. This solution was passed through a cation exchange column (CG50, Sigma) and washed with 500 mL of water and 500 mL of 0.025 M of ammonium hydroxide. The desired product was eluted by 0.25 M of ammonium hydroxide and was lyophilized to yield an orange powder as the product (16 mg, yield 92%). ^{1}H-NMR (D_2O, 500 MHz) δ = 1.348 (q, 1H), 1.795 (q, 1H), 2.027 (m, 1H), 2.159 (m, 1H), 2.889 (m, 1H), 3.097−3.830 (m), 4.893 (d, 1H), 5.319 (d, 1H); aromatic: 6.529 (d, 4H,), 7.047 (m, 2H), 7.317 (d, 1H), 7.805 (d, 1H), 8.071 (s, 1H). FABMS: 826 $(M + H)^+$.

Synthesis of 5-Carboxytetramethylrhodamine Labeled Tobramycin (CRT). To 0.5 mL of water solution of tobramycin (9 mg, 19.3 μmol) was added 0.5 mL of DMF solution containing 5 mg of 5-carboxytetramethylrhodamine (10 μmol). This mixture was then allowed to react at room temperature in the dark for 10 h. Water (10 mL) was added after the reaction was complete. This solution was then passed through a CG-50 column (Sigma, 5 × 30 mm) and washed with 100 mL of water. Crude CRT was eluted with 2 N ammonium hydroxide. The crude product was purified on a C-18 reverse phase column by HPLC (Rainin Instruments). A good separation was achieved using a gradient of acetonitrile/water. The acetonitrile content was increased from 0% to 40% over 40 min. All solvents contained 10 mM trifluoroacetic acid. CRT was concentrated in vacuo and lyophilized. ^{1}H-NMR (D_2O, 500 MHz) δ = 1.884 (q, 1H), 2.005 (m, 1H), 2.274 (m, 1H), 2.467 (m, 1H), 3.165 (s, 6H), 3.370 (t, 1H), 3.470−3.805 (m), 3.911 (t, 1H), 3.982 (q, 1H), 4.964 (d, 1H), 5.607 (d, 1H); aromatic: 6.796 (s, 2H), 6.887 (m, 2H), 7.169 (q, 2H), 7.469 (d, 1H), 7.963 (d, 1H), 8.122 (s, 1H). FABMS: 880 $(M + H)^+$.

Synthesis of the EDTA Linked Tobramycin Analog (ET). Tobramycin (53 mg, 0.11 mmol) was suspended in 0.5 mL of DMF. A few drops of water was added to solubilize the tobramycin. A linker EDTA *N*-hydroxysuccinimide derivative (Taylor et al., 1984) (0.11 mmol, 63 mg) was dissolved in 0.5 mL of DMF and added to the tobramycin solution. The solution was allowed to stir at room temperature for 16 h. At the end of this time, approximately half of the reaction solution was diluted 14 times with water and purified using a CM Sephadex C-25 column (4 × 1 cm). The column had previously been treated with 0.5 M NH_4OH followed by water. The sample was loaded onto the column, and the column was washed with the following solutions: water until the pH of the eluant was again neutral, 0.025 M NH_4OH (27 mL), 0.05 M NH_4OH (30 mL), 0.10 M NH_4OH (50 mL), 0.25 mL of NH_4OH (50 mL), and 0.5 M NH_4OH (50 mL). The coupling product was collected as a colorless oil (24 mg).

The crude triester coupling product was hydrolyzed by treatment with 3.0 mL of 0.5 M LiOH. The solution was stirred at room temperature for 20 h. At the end of this time, the solution was cooled in an ice water bath and neutralized with 10% HCl. The solution was then placed on a CM Sephadex C-25 column that had previously been treated with 0.5 M NH_4OH followed by water. The sample was loaded onto the column, and the column was washed with the following solutions: water until the pH of the eluant was again neutral, 0.0125 M NH_4OH, 0.025 M NH_4OH (20 mL), 0.05 M NH_4OH (20 mL), 0.10 M NH_4OH (20 mL), 0.25 mL of NH_4OH (50 mL), and 0.5 M NH_4OH (50 mL). The product (ET) was collected as a colorless solid (5.2 mg, 9% yield): R_f 0.60 (5:4:3:1 H_2O/CH_3OH/1-butanol/NH_4OH); ^{1}H NMR (500 MHz, D_2O) δ = 1.19 (dd, 1H, J = 14, 7 Hz, -CH_2), 1.90−1.97 (m, 2H), 2.16−2.19 (m, 2H), 2.77−2.81 (m, 1H), 2.88−2.94 (m, 2H), 3.0−3.3 (m, 16H), 3.38−3.51 (m, 3H), 3.59−3.67 (m, 8H), 3.76−3.78 (m, 1H), 4.91 (br s, 1H, anomeric proton), 5.02 (br s, 1H, anomeric proton); mass spectra (FAB positive ion) *m/z* 827 $(M + H)^+$.

RNA Constructs. Preparation of J6-cDNA and J6RNA. A 109-mer ssDNA, GGGAGAATTCCGACCAGAAGCTTAGTATAGCGAGGTTTAGCTACACTCGTGCTGATCGTTTGGTACGGGACCTGCGTGTAGCCCATATGTGCGTCTACATGGATCCTCA, was synthesized. PCR strategy was used to make double-stranded J6-cDNA and to attach the T7 promoter sequence (Wang & Rando, 1995). The two PCR primers are as follows: TGAGGATCCATGTAGACGCACATA (primer 1, 24-mer) and AGTAATACGACTCACTATAGGGAGAATTCCGACCAGAAG (primer 2, 39-mer). PCR conditions: 95 °C for 1 min, 55 °C for 2 min, and 72 °C for 2 min. The PCR product was purified by ethanol precipitation and was resuspended in 50 μL of water. J6RNA was prepared by transcription of J6-cDNA using the T7-MEGAshortscript kit. Template J6-cDNA was degraded by RNase-free DNase I, provided with the kit. RNA was purified by Sephadex G-50 gel filtration using a prepacked column (NICK columns). RNA concentrations were determined spectroscopically at 260 nm.

The X1 and X3 RNAs were prepared by the method described above for J6, as previously reported (Wang & Rando, 1995). 3′-End labeling of the RNA constructs with [5′-^{32}P]cytidine 3′,5′-bisphosphate was carried out using T4 ligase by the published procedure ((England et al., 1980).

Fluorescence Intensity and Polarization Measurements. Fluorescence intensity and polarization measurements were performed on a LS-50B spectrofluorimeter (Perkin Elmer) at 20.0 ± 0.1 °C. Samples were excited at 490 nm, and fluorescence was monitored at 525 nm (CFT) or 582 nm (CRT). Slits on both excitation and emission sides were 10 nm for CFT and 15 nm for CRT. Integrated times for both fluorescence intensity and polarization measurements are 4 s. For every single point, 4−6 measurements were made, and their average value was used for calculations. In general, the errors were less than 0.5% for the fluorescence intensity measurements and less than 0.0020 for fluorescence anisotropy measurements. Measurements were made in a buffer containing 140 nM NaCl, 5 mM KCl, 1 mM $MgCl_2$, 1 mM $CaCl_2$, and 20 mM HEPES (pH 7.40). CFT and CRT concentrations were determined spectroscopically at 492 and 550 nm, respectively, using the molar extinction coefficients 7.80×10^4 and 6.00×10^4 cm^{-1} M^{-1}, respectively.

Determination of Binding Parameters. The affinity of J6RNA for the dye labeled tobramycin was determined by fluorescence anisotropy measurements. The fraction of

fluorescence intensity (F) due to the bound species is given by:

$$F = (A - A_f)/(A_b - A_f) \quad (1)$$

where A, A_b, and A_f are the anisotropy values of sample, totally bound tracer (tr), and totally free tr, respectively. In cases where both the bound and free fluorophores have the same level of fluorescence intensity, the mole fraction of bound tr (f) is the same as F. However, if the bound tr has a different intensity from free tr, the following equation is used to obtain f:

$$f = F/(1 + Q(1 - F)) \quad (2)$$

where Q is the fluorescence intensity enhancement factor, determined by the intensity measurement. A_0 (i.e., $[T]_0$) refers to the total concentration of a given molecule.

$$\text{RNA·tr} \rightleftharpoons \text{RNA} + \text{tr} \quad (3)$$

$$[\text{RNA·tr}] = [\text{tr}]_0 f \quad (4)$$

$$[\text{tr}] = [\text{tr}]_0(1 - f) \quad (5)$$

$$[\text{RNA}] = K_D[\text{RNA·tr}]/[\text{tr}] \quad (6)$$

$$[\text{RNA}]_0 = [\text{RNA}] + [\text{RNA·tr}] \quad (7)$$

From eqs 1−7, we obtain:

$$[\text{RNA}]_0 = [K_D(A - A_f)/((1 + Q)(A_b - A))]/[[\text{tr}]_0(A - A_f)/((1 + Q)A_b - A)] + (A - A_f)/((1 + Q)(A_b - A)) \quad (8)$$

Equation 8 was used for the calculation of K_D, the dissociation constant for the fluorescent tracer (tr).

The affinities of J6RNA for tobramycin (T) and other antibiotics (T) were determined by competition with the fluorescent tracers (tr).

$$\text{RNA·tr} \rightleftharpoons \text{RNA} + \text{tr} \quad (3)$$

$$\text{RNA·T} \rightleftharpoons \text{RNA} + \text{T} \quad (9)$$

$$[\text{RNA·tr}] = [\text{tr}]_0 f \quad (4)$$

$$[\text{tr}] = [\text{tr}]_0(1 - f) \quad (5)$$

$$[\text{RNA}] = K_D[\text{RNA·tr}]/[\text{tr}] \quad (6)$$

$$[\text{T}] = K_{D*}[\text{RNA·T}]/[\text{RNA}] \quad (10)$$

$$[\text{RNA}]_0 = [\text{RNA·T}] + [\text{RNA}] + [\text{RNA·tr}] \quad (11)$$

$$[\text{T}]_0 = [\text{T}] + [\text{RNA·T}] \quad (12)$$

The following equation is derived from the preceding:

$$[\text{T}]_0 = (K_{D*}/(K_D(A - A_f)/((1 + Q)(A_b - A))) + 1) \times ([\text{RNA}]_0 - (K_D(A - A_f)/((1 + Q)(A_b - A))) - [\text{tr}]_0(A - A_f)/((1 + Q)A_b - A_f - QA)) \quad (13)$$

RESULTS

Affinity Cleavage of Tobramycin Binding Aptamers Occurs in the Consensus Domains. As described previously, stringent selection of tobramycin binding aptamers revealed two closely related consensus sequences (Wang & Rando, 1995). This would suggest that the consensus sequences are important parts of the tobramycin binding sites. To prove this, we prepared and studied the EDTA−tobramycin-based affinity cleaving agent ET shown in Chart 1. Affinity cleaving agents of this type make use of the well-known ability of Fe^{2+}/EDTA/thiol complexes to affinity cleave DNA (Taylor et al., 1984) and RNA (Prudent et al., 1995). In the current work, it would be expected that ET would cleave tobramycin binding aptamers in their tobramycin binding sites.

Chart 1: Structure of the Tobramycin-Based RNA Cleaving Agent

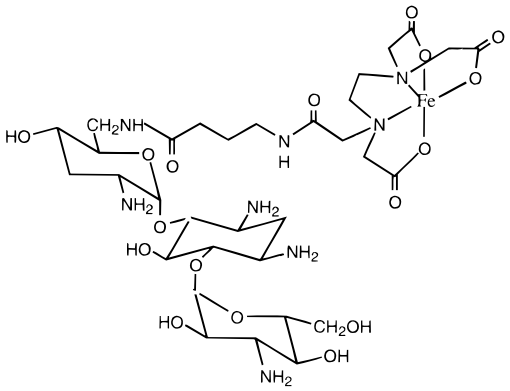

EDTA-Tobramycin (ET)

The synthesis of ET relies on the fact that the 6′-amino group of tobramycin can be preferentially acetylated, since it is the only unhindered primary amino group in the molecule (Tangy et al., 1983). Thus, tobramycin can be readily modified at its 6′-amino group by acylation with *N*-hydroxysuccinimide ester of pyrenebutyric acid to provide 6′-*N*-(4-pyrenebutyryl)tobramycin (PYT) (Wang & Rando, 1995). A similar synthetic procedure was used to prepare the EDTA-based derivative (ET) shown in Chart 1. Three tobramycin binding aptamers, whose random region sequences are recorded below (consensus sequences in bold), were selected for further study:

5′...CUGGUUAGUUUUGCACAGUGGTCGA-
UGCUAGACU**UGGUUUA**GG**UAAUG**AGUCCAA-
UAGUC...3′ (**X1**)

5′...AGUAUAGCG**AGGUUUA**G**CUACACU**C-
GUGCUGAUCGUUUGGUACGGGACCUGCGUG-
UAGCC...3′ (**J6**)

5′...UGGUUGUCUUGUACGUUCACUGUUACG-
AUUGUGUU**AGGUUUA**A**CUACACU**UUGCA-
AUCG...3′ (**X3**)

These aptamers also contain the following 5′ and 3′ primer sequences: 5′-GGGAGAAUUCCGACCAGAAGCUU-random region-CAUAUGUGCGUCUACAUGGAUCCUCA-3′. In Chart 2 are shown Mfold (Jaeger et al., 1989) minimized structures of the three aptamers with the indicated consensus regions. In order to determine if the consensus regions comprised part, or all, of the tobramycin binding sites, the three constructs were incubated with the tobramycin−EDTA (ET) analog to determine whether cutting occurred in the consensus regions. In Figure 1 are shown gels for the

Chart 2: Minimized Structures for X1, X3, and J6[a]

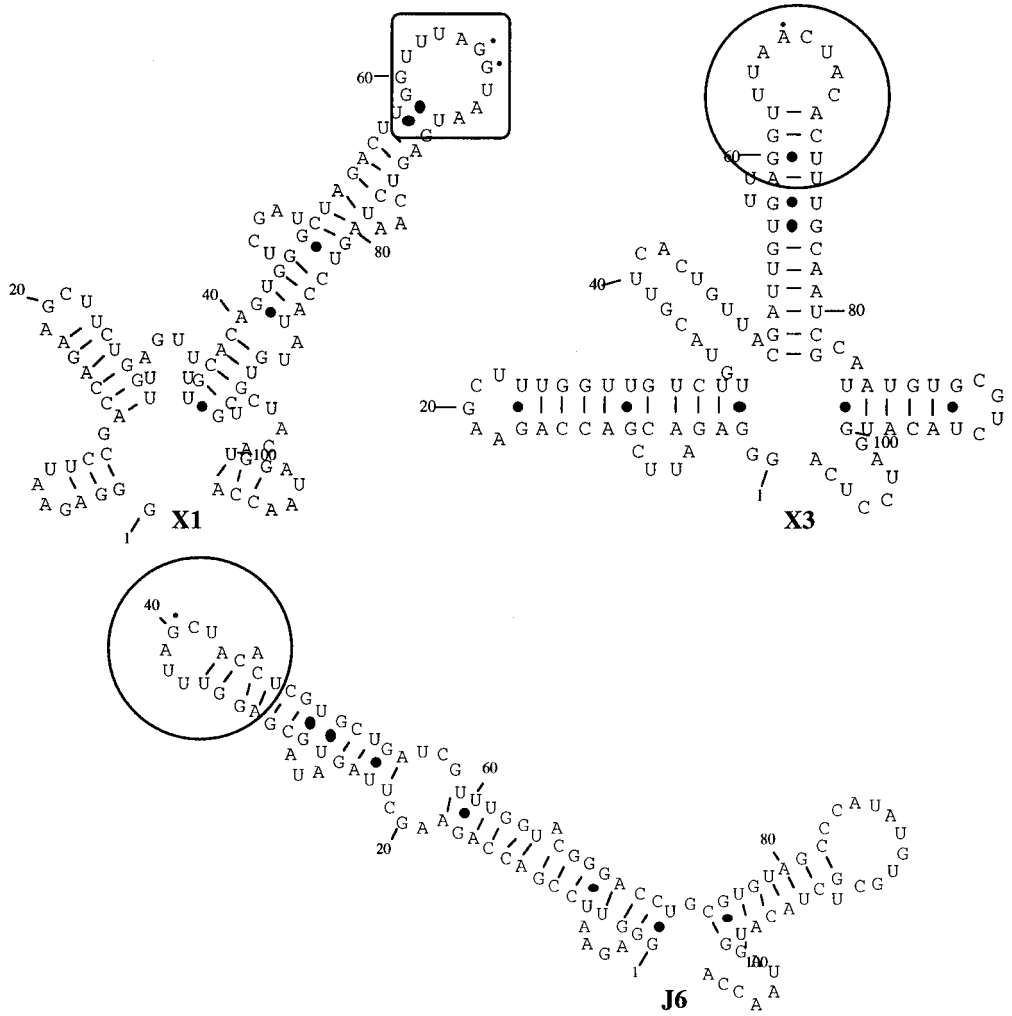

[a] Outlined areas indicate consensus regions. The bold dots indicate wobble base pairs, and the small dots in the outlined areas indicate nonconsensus bases.

cleavage of 3′-^{32}P end labeled J6 (lanes 1−6), 3′-^{32}P end labeled X1 (lanes 8−13), and 3′-^{32}P end labeled X3 (lanes 15−20) at increasing concentrations of ET. Lanes 7, 14, and 21 show cutting by the A-selective RNase U2. As can be seen in these gels, RNA cutting is specific at low concentrations of drug, and the cutting is confined to the consensus regions of the constructs. At high concentrations of drug (>1 μM), nonspecific cleavage of the constructs occurs. Figure 2 shows a time course for the cleavage of J6 by ET, this time with the G selective RNase T1 shown in lane 7. Clear cleavage in the consensus region can be seen at the first time point (15 min) and increases as a function of time through the last time point at 2 h. To further demonstrate that cleavage occurs in the consensus regions, the cleavage of J6 is studied in the presence of tobramycin, neomycin, and erythromycin (Figure 3). In Figure 3 are shown potent inhibition of ET-induced affinity cleavage by tobramycin (lanes 1−7), virtually no inhibition of cutting by the non-aminoglycoside antibiotic erythromycin (lanes 8−12), and moderate competition by the aminoglycoside neomycin (lanes 13−17). As will be demonstrated later, J6 exhibits basically no affinity for erythromycin and binds neomycin approximately 1000-fold less avidly than it binds tobramycin. These experiments demonstrate that the affinity cutting occurs in the aminoglycoside binding region and that this binding region is largely defined by the consensus region. Finally, to demonstrate that affinity cleavage caused by ET requires the tobramycin moiety, cleavage of J6 by this reagent is compared to cleavage caused by Fe^{2+}/EDTA/DTT (Figure 4). As shown in Figure 4, Fe^{2+}/EDTA/thiol-mediated cleavage occurs only at high concentrations of the reagents and is nonspecific as well, demonstrating that the tobramycin moiety is essential for affinity cleavage.

Binding Characteristics of Dye-Labeled Tobramycins with J6RNA. An important issue to address in studying RNA aptamers is how to quantitatively determine what the specificity and stoichiometry of ligand binding is. To these ends, a fluorescence depolarization was sought which would provide accurate binding data in both direct and competitive binding assays. Initial experiments were performed to determine if CFT and CRT, whose structures are shown below, exhibit fluorescence anisotropy changes upon binding to J6RNA. Tobramycin is reacted with 5-carboxyfluorescein succinimidyl ester or 5-carboxytetramethylrhodamine succinimidyl ester to generate the two fluorescent probes used in this work, CFT and CRT (Chart 3).

Binding studies were carried out by titration of a solution of CFT or CRT (10.0 nM) (Chart 3) with aliquots of J6RNA stock solution. J6RNA had previously been prepared by selecting random RNA pools against a tobramycin affinity column (Wang & Rando, 1995). Figure 5A,B shows the change in fluorescence anisotropy as a function of J6RNA

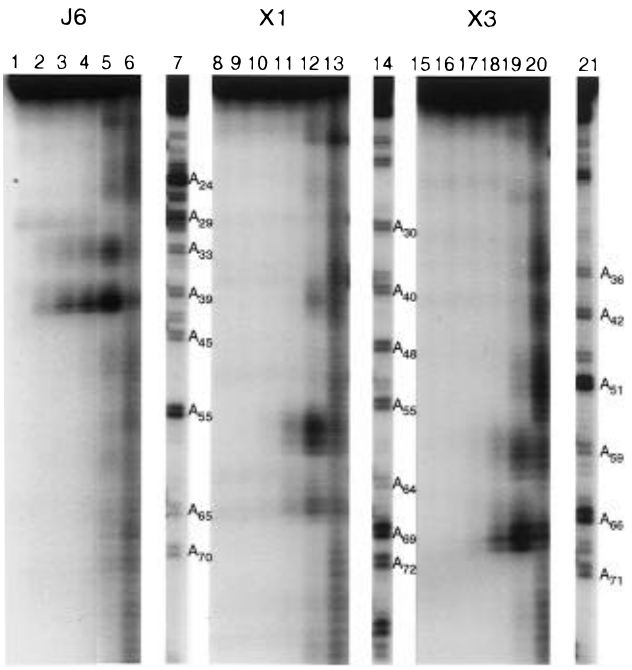

FIGURE 1: Affinity cleavage of J6, X1, and X3 by Fe(II)·ET. The RNA constructs were cleaved for 2 h at 42° C in the presence of 1 mM DTT and 520 ng of carrier to RNA from bakers' yeast. 1 mL of A-(U2) or G-selective (T1) RNases were added in lanes 7, 14, and 21. For J6 cleavage: (lanes 1−6) +0, 10 nM, 100 nM, 1 μM, 10 μM Fe(II)·ET; (lane 7) A lane; RNase U2 added. For X1 cleavage: (lanes 8−13) +0, 10 nM, 100 nM, 1 μM, 10 μM, 100 μM Fe(II)·ET; (lane 14) A lane; RNAase U2 added. For X3 cleavage: (lanes 15−20) +0, 10 nM, 100 nM, 1 μM, 1 μM, 10 μM, 100 μM Fe(II)·ET; (lane 21) A lane; RNase U2 added.

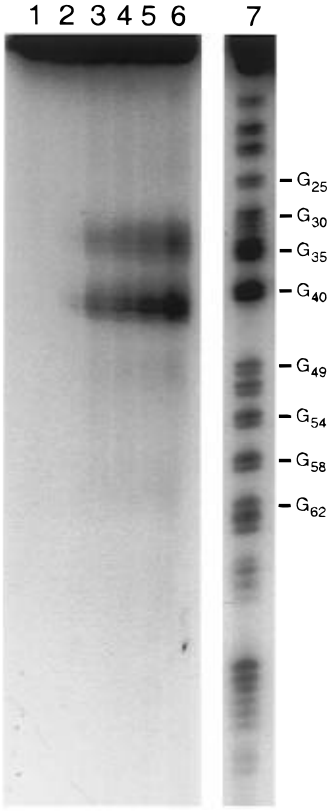

FIGURE 2: Time course for the cleavage of J6 by Fe(II)·ET. The conditions for cleavage were the same as indicated in Figure 1. (Lanes 1−6) −ET, t = 0; +ET, t = 0; +ET, t = 15 min; +ET, t = 30 min; +ET, t = 1 h; +ET, t = 2 h; (lane 7) G lane for J6; RNase T1 added.

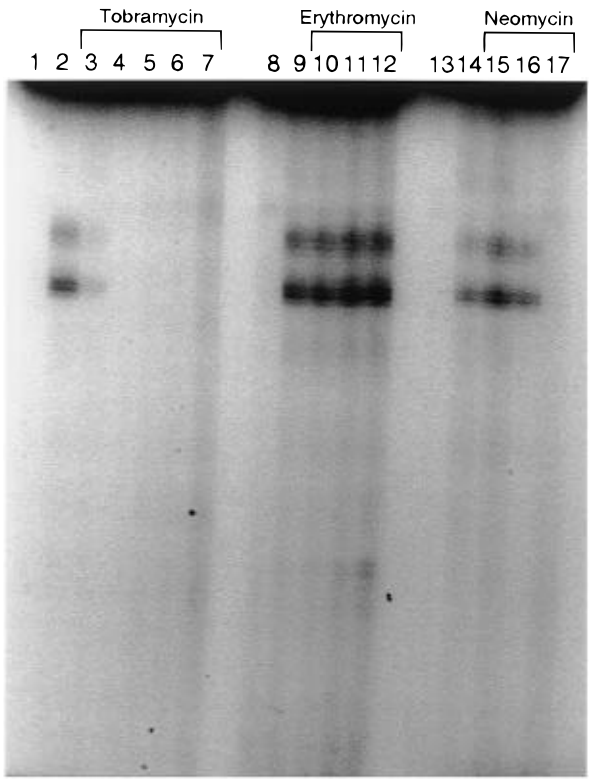

FIGURE 3: Inhibition of Fe(II)·ET-mediated cleavage of J6 RNA by tobramycin, erythromycin, and neomycin B. The conditions for cleavage were the same as indicated in Figure 1. (Lane 1) J6RNA only; (lanes 2−7) +0 (0×); 2.1 μM (1×); 10.4 μM (5×); 50 μM (25×); 260 μM (625×); 1.3 μM (3125×) concentrations of tobramycin; (lane 8) J6 RNA alone; (lanes 9−12) +0 (0×); 2.1 μM (1×); 10.4 μM (5×); 50 μM (25×) concentrations of erythromycin; (lane 13) J6RNA only; (lanes 14−17) +0 (0×); 2.1 μM (1×); 10.4 μM (5×); 50 μM (25×) concentrations of neomycin B.

concentrations for CFT and CRT, respectively. Fluorescence intensities of the mixtures, measured as a function of increasing RNA concentrations, showed no significant change in the emission intensity for CFT, and a small change for CRT. The fluorescence enhancement factor (Q) was measured as 0 for CFT and 0.11 for CRT at saturating RNA concentrations. The anisotropy values in the absence of J6RNA (A_0) were 0.0230 ± 0.0005 and 0.0420 ± 0.0014 for CFT and CRT, respectively. Addition of J6RNA resulted in a gradual increase in anisotropy. The anisotropy values for completely bound CFT and CRT (A_b) were 0.0493 ± 0.0006 and 0.1041 ± 0.0018, respectively. The significant increase in anisotropy was attributed to the large difference in molecular size between the free dye-labeled tobramycins (ca. 800 Da) and their RNA complexes (ca. 360 000 Da), and this difference is large enough to allow binding to be quantified. The above values of Q, A_f, and A_b were used in conjunction with eq 8 (Methods section) to calculate dissociation constants (K_D's) for the binding of CFT and CRT (denoted as tr in the equations derived in Methods) to J6RNA. Plots of $[RNA]_0$ vs A are given in Figure 5A,B, and dissociation constants of 114 ± 6.4 nM and 12.3 ± 1.1 nM are determined for CFT and CRT, respectively. The experimental data fit the calculated curves quite well in Figure 5A,B, demonstrating that the stoichiometries of ligand binding are 1:1. The equations derived in Methods all assume a 1:1 stoichiometry.

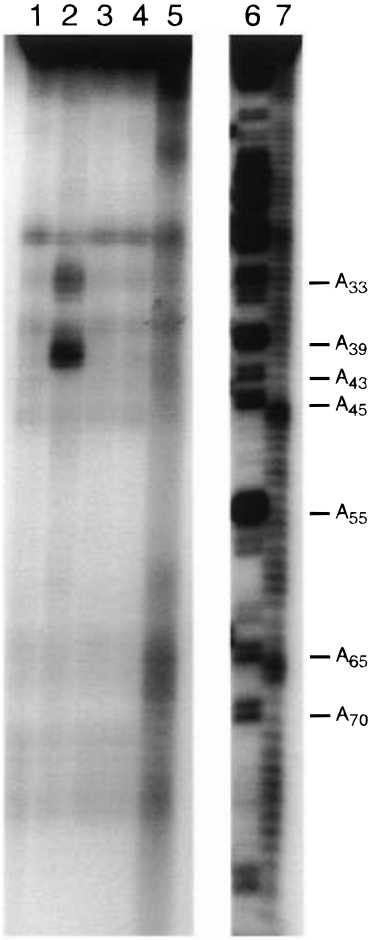

FIGURE 4: Cleavage of J6 by Fe(II)/EDTA and Fe(II)·ET. Cleavage conditions in these experiments were the same as indicated in Figure 1. (Lane 1) J6RNA alone; (lane 2) +2 μM Fe(II)·ET; (lane 3) +2 μM Fe(II)·EDTA; (lane 4) +2 μM ET-Fe^{2+}, −DTT; (lane 5) +1 mM Fe(II)·EDTA; (lane 6) A lane; RNase U2 added; (lane 7) base hydrolysis lane.

Chart 3: Structures of CFT and CRT

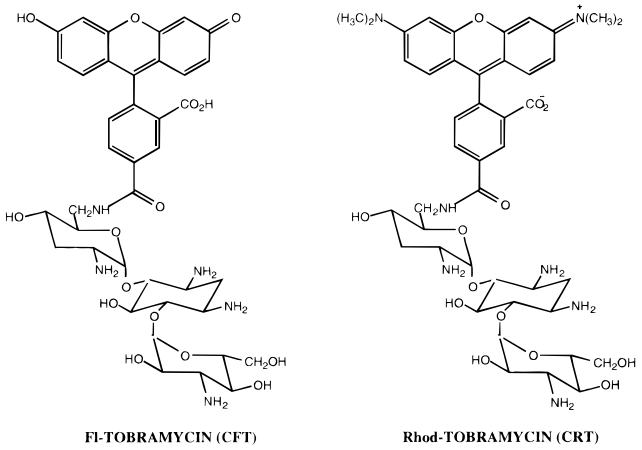

The above results show that CRT is a much more promising probe than CFT for quantitative binding measurements, because of the larger anisotropy change measured upon binding to J6RNA, and because of CRT's inherently higher affinity for the RNA construct. Thus, in all further experiments described here, CRT is utilized as the binding probe.

Competitive Binding of Tobramycin with CRT. Reversibility of binding is one critical factor determining the utility

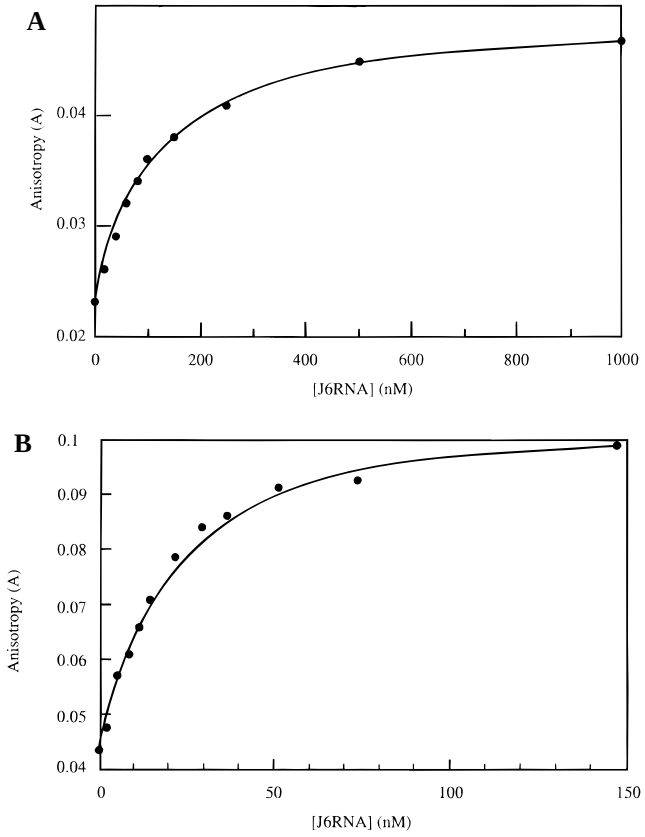

FIGURE 5: (A) Fluorescence anisotropy (*A*) of CFT solutions (10.0 nM) as a function of J6RNA concentrations. The solid line is calculated by curve fitting of the experimental data to eq 8. The dissociation constant was measured to be 114 nM. (B) Fluorescence anisotropy (*A*) of CRT solutions (10.0 nM) as a function of J6RNA concentrations. The solid line is calculated by curve fitting of the experimental data to eq 8. The dissociation constant was measured to be 12.3 nM.

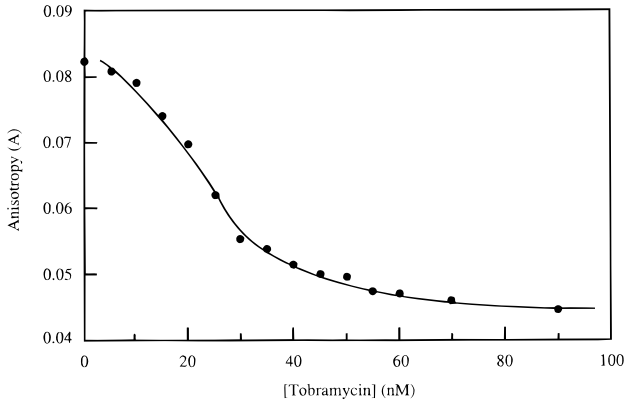

FIGURE 6: Fluorescence anisotropy (*A*) of CRT solutions (10.0 nM) containing J6RNA (28 nM) as a function of tobramycin concentration. The solid line is calculated by curve fitting of the experimental data to eq 17. The dissociation constant for tobramycin was found to be 0.77 nM.

of CRT as a probe to monitor aminoglycoside binding to J6RNA. In initial experiments, tobramycin was used to displace the CRT from J6RNA. A mixture of CRT (10.0 nM) and J6RNA (30 nM) was first prepared. The starting anisotropy value was measured to be 0.0810 ± 0.0020. Displacement experiments were carried out by adding aliquots of tobramycin to the mixture. Figure 6 shows that as the tobramycin concentration was increased, the anisotropy gradually decreased, approaching that of free CRT. Using

Table 1: Dissociation Constants of J6RNA (20 °C)

	antibiotics				
	CRT	tobramycin	neomycin B	gentamycin C	erythromicin
K_D (μM)	0.0123 ± 0.0011	0.00077 ± 0.00003	1.03 ± 0.03	7.81 ± 0.54	923 ± 49

data in Figure 6 and $K_D = 12.3$ nM, it was also possible to obtain the dissociation constant of tobramycin with respect to the RNA. Nonlinear curve fitting, following eq 17 (Methods), gave a $K_{D*} = 0.77 \pm 0.03$ nM. Thus, tobramycin binds 16-fold more tightly to J6RNA than does CRT. This suggests that the tetramethylrhodamine B moiety in the CRT interferes with the interaction between tobramycin and the RNA. Using data in Figure 6, we can also calculate both K_D and K_{D*}. Without using the value of K_D, nonlinear curve fitting according to eq 17 gave a $K_D = 12.9 \pm 1.2$ nM and $K_{D*} = 0.81 \pm 0.09$ nM. This value of K_D is in excellent agreement with that obtained from the direct anisotropy measurement (Figure 5B). Since the K_D values calculated by the two independent measurements are in excellent agreement, it follows that tobramycin and the fluorescent probes quantitatively compete for binding to the RNA construct.

Competitive Binding of Neomycin B, Gentamycin, and Erythromycin with CRT. With this new assay in hand, it was of interest to investigate the specificity of J6RNA/drug binding. Competitive binding experiments were performed with three other antibiotics—neomycin B, gentamycin C, and erythromycin. Neomycin B and gentamycin C are aminoglycoside antibiotics thought to interfere with protein synthesis by specifically binding to procaryotic rRNA (Gale et al., 1981). Diverse aminoglycosides have also been reported to bind to and block the function of other RNA molecules, including group I introns (von Ahsen et al., 1991), HIV RRE RNA (Zapp et al., 1993), and a hammerhead ribozyme (Stage et al., 1995). Erythromycin is a macrolide antibiotic which inhibits protein synthesis but is structurally unrelated to the aminoglycosides (Gale et al., 1981).

Competitive binding experiments were performed under the same conditions as previously described with tobramycin. Neither neomycin B, gentamycin C, nor erythromycin displaced CRT from its J6RNA complex at low ligand concentrations. They only displace CRT at very high concentrations. This indicates that the binding of J6RNA is very specific for tobramycin. The affinities of neomycin B, gentamycin C, and erythromycin for J6RNA were calculated using data from competitive binding experiments involving high concentrations of competitors; these data are reported in Table 1. Figure 7 shows the competitive experiment data and the nonlinear curve fitting plot for the calculation of the K_D for neomycin B. The affinity of J6RNA for tobramycin is 1338 times greater than that for neomycin B, 10 143 times greater than that for gentamycin C, and 1198 000 times greater than that for erythromycin.

Fluorescence Polarization Assay. The specificity and affinity of binding of J6RNA for tobramycin suggest that J6RNA could be used to assay tobramycin levels quantitatively. A standard curve for a typical fluorescence polarization assay in which a mixture of 10 nM CRT and 28 nM J6RNA was titrated by aliquots of tobramycin is shown in Figure 8A. The sensitivity (*S*) was defined as the tobramycin concentration which corresponds to 1.96 times the standard deviation of the polarization value obtained in the absence

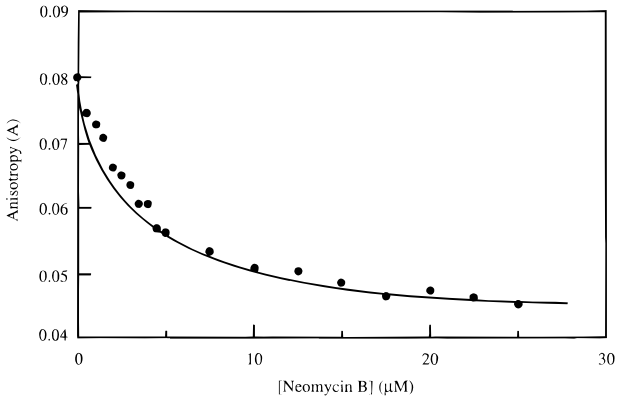

FIGURE 7: Fluorescence anisotropy (*A*) of CRT solutions containing (10.0 nM) J6RNA (28 nM) as a function of neomycin B concentrations. The solid line is calculated by curve fitting of the experimental data to eq 17. The dissociation constant for neomycin B was measured to be 1.03 μM.

of tobramycin. In this case, *S* was found to be 1.3 ng/mL (2.8 nM). The value for a commercially used immunopolarization assay for tobramycin is approximately 150 greater (Chan, 1987), demonstrating the enormous sensitivity enhancement available with J6RNA relative to protein antibodies. As shown in Figure 8B, the assay operates in a linear manner over substantial ranges of tobramycin concentrations (2−14 ng/mL in Figure 8B), making it potentially quite useful for assaying tobramycin levels. By varying the concentrations of RNA and probe, the linearity of the response could be substantially increased if desired.

DISCUSSION

In a previous study, we had reported that RNA aptamers could be selected against the aminoglycoside antibiotic tobramycin (Wang & Rando, 1995). A group of aptamers which had a high affinity for tobramycin all contained consensus sequences (Wang & Rando, 1995). Chart 2 indicates Mfold minimized (Jaeger et al., 1989) secondary structural predictions for three such representative aptamers (X1, X3, and J6), as well as indicating the consensus sequences. The fact that consensus sequences are predicted to appear in stem-loop structures suggests the possibility that the consensus regions define at least part of the tobramycin binding site. To test this hypothesis directly, tobramycin-based affinity cleaving agents were developed (Chart 1). One of these reagents (ET) was studied in detail. At low concentrations, the reagent specifically cleaved X1, X3, and J6 in their respective consensus regions (Figure 1). The tobramycin moiety is important, because Fe^{2+}/EDTA/DTT only cuts nonspecifically under relative forcing conditions. In addition, affinity cleavage by ET could be effectively blocked by tobramycin, but not by erythromycin, which has only a very weak affinity for J6 (Figure 3, Table 1). Neomycin B, which binds to J6 with a greater than 1000-fold lower affinity compared to tobramycin, weakly protected against cleavage caused by ET. These experiments show that the tobramycin binding site is defined largely, if not

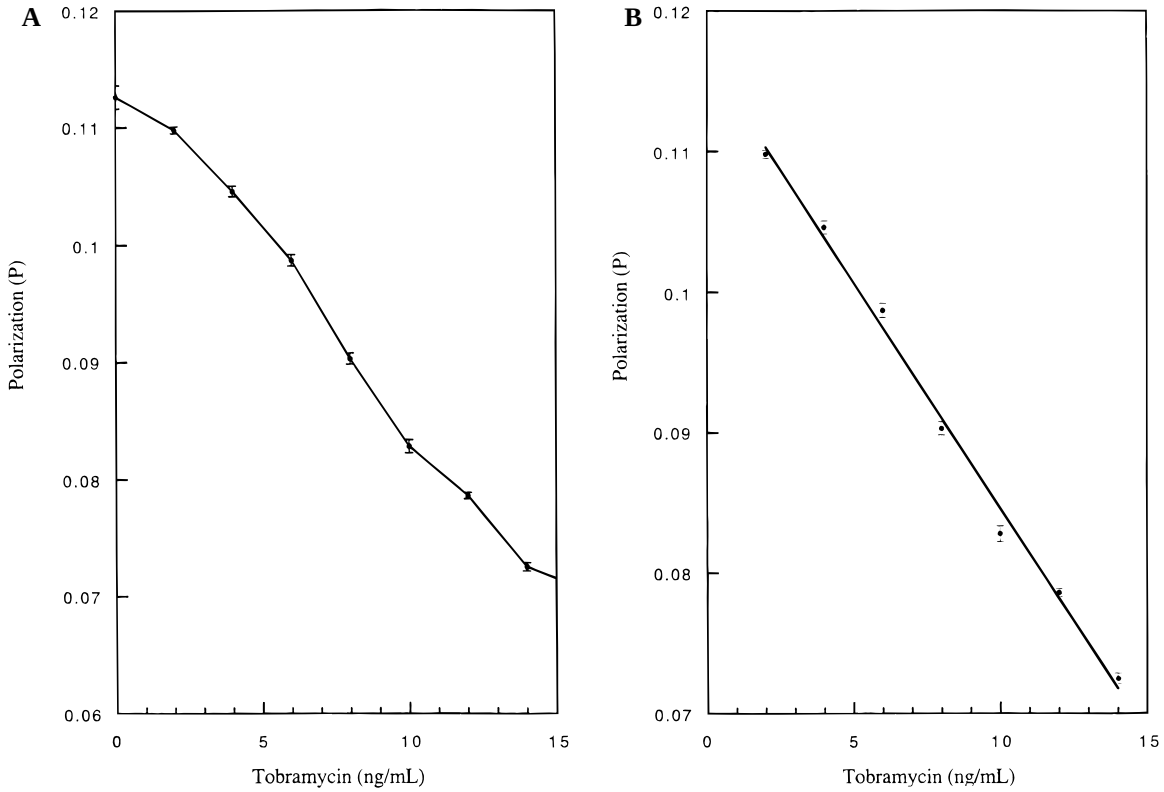

FIGURE 8: (A) Standard curve of a typical of J6RNA system. Aliquots of a tobramycin stock solution were added to a mixture of J6RNA (25 nM) and CRT (10.0 nM). Error bars represent the standard deviation of three separate experiments. (B) Linear response region of J6RNA.

Chart 4: Structures of Tobramycin and 6′-*N*-(Pyrenebutyryl)tobramycin

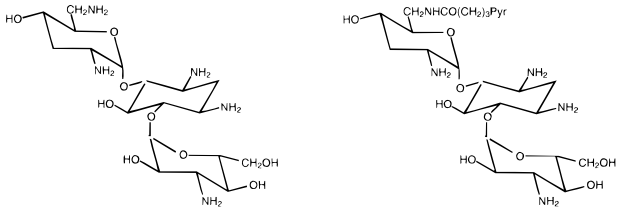

entirely, by predicted stem-loop regions. This idea is supported by the fact that the consensus binding regions appear at different places in the various aptamers, suggesting that the remainder of the aptamer structure is relatively unimportant for aminoglycoside binding.

The experiments described above show that the tobramycin binding sites are largely confined to the consensus regions and are probably found in stem-loop structures. In studying these RNA aptamers, it is also important to develop quantitative tools for the determination of affinities and specificities of ligand binding. Previously, we had shown that the pyrenebutyramide derivative of tobramycin shown in Chart 4 (PYT) binds to RNA tobramycin binding aptamers, such as J6, with an affinity similar to that of tobramycin itself (Wang & Rando, 1995). The binding could be readily followed by fluorescence quenching, because the fluorescence of PYT was quenched as a consequence of binding to the RNA (Wang & Rando, 1995). However, pyrene itself has a significant affinity for DNA as an intercalating agent, estimated to be in the mM range (Boyland & Green, 1962). It is probable that pyrene can also intercalate with double-stranded regions of RNA with similar affinities. When coupled to the weak, nonspecific binding of an aminoglycoside to RNA, which easily could be in the micromolar to 0.1 μM range, the possibility of measuring nonspecific binding is a serious problem. Thus, in the case of PYT, a second low-affinity binding constant could be measured (Wang & Rando, 1995). This low-affinity binding is probably relatively nonspecific and confounds the quantitative analysis of aminoglycoside binding to RNA aptamers, because the relative amount of quenching in the two binding modes is indeterminate. It was therefore imperative to develop a new quantitative assay system to measure the specific binding of ligands to RNA aptamers accurately and conveniently. It is probable that any fluorescence probe which is quenched upon binding to RNA is likely to interact with it, resulting in the possibility of nonspecific interactions. To circumvent this difficulty, a fluorescence methodology was sought which did not require that the fluorescent moiety interact with the RNA, as required in a quenching measurement. Fluorescence depolarization methods seemed ideal, because the probe need not interact with the RNA. Fluorescein and tetramethylrhodamine analogs were chosen because of their high extinction coefficients and quantum yields for fluorescence. Furthermore, the fluorescent moieties are either neutral or negatively charged and would not be expected to interact strongly with the RNA.

The 5-carboxytetramethylrhodamine analog of tobramycin (CRT) proved to be the most useful fluorescence probe both because it binds to J6RNA with high affinity, and because a reasonably large anisotropy change occurs as a consequence of CRT binding to J6RNA. Using this new assay system, the binding of CRT to J6RNA showed only stoichiometric binding at high affinity. Competition experiments with neomycin, gentamycin, and erythromycin, shown in Chart

Chart 5: Structures of Antibiotics Used as Competitive Inhibitors

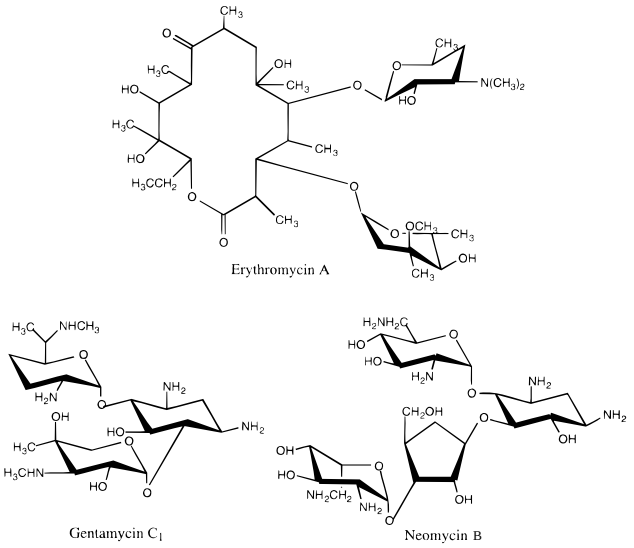

5, demonstrated that J6RNA is extremely selective and discriminates by factors of 1338, 10 143, and 1198 000 as compared to the binding of tobramycin to neomycin, gentamycin, and erythromycin, respectively. It is interesting to note that nowhere near this discrimination has been demonstrated in the binding of aminoglycosides to various other RNA molecules, including introns, HIV-1 RRE RNA, and hammerhead ribozymes (von Ahsen et al., 1991; Zapp et al., 1993; Stage et al., 1995). In these other instances, the binding affinities for the aminoglycosides are probably in the 0.1−10 μM range and are hence not likely to be highly specific in nature. This suggests that the J6RNA construct will be useful for understanding the rules underlying specific RNA−aminoglycoside recognition.

The high affinity and specificity of J6RNA for tobramycin suggests that it could be used to measure low levels of the antibiotic. Because of their toxicities, aminoglycosides are often clinically monitored during therapy (Chan, 1987). Interestingly, the J6RNA construct is able to measure tobramycin levels accurately in the 0−15 ng/mL (0−28 nM) range. This assay is approximately 150-fold more sensitive than extant fluorescence polarization immunoassays for measuring aminoglycoside levels (Chan, 1987). Moreover, the assay is linear over an extensive concentration range of tobramycin, enhancing its utility. This work suggests an unanticipated application for RNA aptamers: they may be useful in clinically-based assays.

REFERENCES

Altman, S. (1989) *Adv. Enzymol. 62*, 1−36.
Beaudry, A., & Joyce, G. F. (1992) *Science 257*, 635−641.
Boyland, E., & Green, B. (1962) *Br. J. Cancer 16*, 507−517.
Cech, T. R. (1990) *Annu. Rev. Biochem. 59*, 543−568.
Chan, D. W. (1987) *Immunoassay Automation: A Practical Guide*, p 332, Academic Press, New York.
Ellington, A. D., & Szostak, J. W. (1990) *Nature 346*, 818−822.
England, T. E., Bruce, A. G., & Uhlenbeck, O. C. (1980) *Methods Enzymol. 65*, 65−75.
Gale, E. F., Cundliffe, E., Reynolds, P. E., Richmond, M. H., & Waring, M. J. (1981) *The Molecular Basis of Antibiotic Action*, Chapter 6, Wiley, New York.
Jaeger, J. A., Turner, D. H., & Zuker, M. (1989) *Methods in Enzymol. 183*, 281−306.
Prudent, J. R., Staunton, J., & Schultz, P. G. (1995) *J. Am. Chem. Soc. 117*, 10145−10146.
Stage, T. K., Hertel, K. J., & Uhlenbeck, O. C. (1995) *RNA 1*, 95−101.
Tangy, F., Capmau, M.-L., & LeGoffic, F. (1983) *Eur. J. Biochem. 131*, 581−587.
Taylor, J. S., Schultz, P. G., & Dervan, P. B. (1984) *Tetrahedron 40*, 457−465.
Tuerk, C., & Gold, L. (1990) *Science 249*, 505−510.
von Ahsen, U., Davies, J., & Schroeder, R. (1991) *Nature (London) 353*, 368−370.
Wang, Y., & Rando, R. R. (1995) *Chem. Biol. 2*, 281−290.
Woodcock, J., Moazed, D., Cannon, M., Davies, J., & Noller, H. F. (1991) *EMBO J. 10*, 3099−3103.
Zapp, M. L., Stern, S., & Green, M. R. (1993) *Cell 74*, 969−978.

BI960878W